

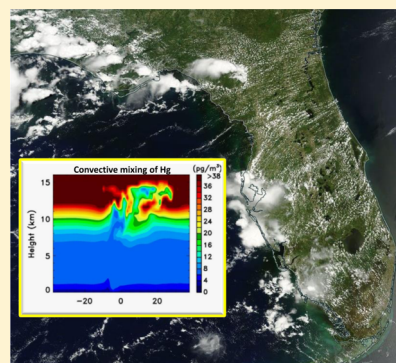
# Mercury Wet Scavenging and Deposition Differences by Precipitation Type

Aaron S. Kaulfus,<sup>\*,†</sup> Udaysankar Nair,<sup>†</sup> Christopher D. Holmes,<sup>‡</sup> and William M. Landing<sup>‡</sup>

<sup>†</sup>Department of Atmospheric Science, University of Alabama in Huntsville, Huntsville, Alabama 35806, United States

<sup>‡</sup>Department of Earth, Ocean and Atmospheric Science, Florida State University, Tallahassee, Florida 32306, United States

**ABSTRACT:** We analyze the effect of precipitation type on mercury wet deposition using a new database of individual rain events spanning the contiguous United States. Measurements from the Mercury Deposition Network (MDN) containing single rainfall events were identified and classified into six precipitation types. Mercury concentrations in surface precipitation follow a power law of precipitation depth that is modulated by precipitation system morphology. After controlling for precipitation depth, the highest mercury deposition occurs in supercell thunderstorms, with decreasing deposition in disorganized thunderstorms, quasi-linear convective systems (QLCS), extratropical cyclones, light rain, and land-falling tropical cyclones. Convective morphologies (supercells, disorganized, and QLCS) enhance wet deposition by a factor of at least 1.6 relative to nonconvective morphologies. Mercury wet deposition also varies by geographic region and season. After controlling for other factors, we find that mercury wet deposition is greater over high-elevation sites, seasonally during summer, and in convective precipitation.



## INTRODUCTION

Atmospheric mercury is a toxic pollutant that causes nervous system disorders in humans and wildlife and is especially harmful during gestational development and childhood.<sup>1–3</sup> Human exposure to mercury occurs primarily through consumption of fish and rice,<sup>4,5</sup> with deposition of atmospheric mercury being the main source of mercury to most marine and aquatic ecosystems. Thus, it is important to understand the transport and fate of atmospheric mercury. In this context, there is a need to understand processes responsible for the observed geographical patterns of mercury wet deposition.

Within the continental United States, the eastern United States and especially the Ohio River Valley have the highest density of atmospheric mercury emissions (Figure 1). In this area, local emissions account for a large fraction of observed mercury wet deposition.<sup>6–8</sup> However, the highest mercury wet deposition in the continental United States occurs along the Gulf Coast, where local emissions are lower than in the Ohio River Valley. Even higher wet deposition is observed in Puerto Rico,<sup>9</sup> an island with no substantial mercury emissions. While Hg deposition is generally low in the arid western United States, concentrations in rain can be high.<sup>10</sup> The discrepancy between local emissions and wet deposition patterns suggests the importance of long-range and global atmospheric mercury cycling in depositing mercury to these regions.<sup>11–13</sup>

Mercury exists in the atmosphere in three forms: gaseous elemental mercury (GEM), gaseous oxidized mercury (GOM), and oxidized particle-bound mercury (PBM). The oxidized species collectively comprise Hg(II). The majority of atmospheric mercury (95%) exists as GEM, which has low solubility and high volatility compared to the oxidized forms.

Due to its low solubility and slow chemical oxidation, GEM has a long atmospheric residence time (0.5–1 year)<sup>14,15</sup> and can be transported globally. The oxidized species are quickly removed from the lower troposphere by dry and wet deposition, but oxidized mercury can accumulate in the upper troposphere and stratosphere.<sup>11,16–24</sup>

Prior studies suggest that this high-altitude reservoir of oxidized mercury could sustain high mercury deposition in regions without significant mercury emissions. Since the reservoir is thought to be widespread in the upper troposphere and lower stratosphere, deposition from it is likely determined by patterns of subsidence and precipitation.<sup>11,25</sup> Although the stratosphere contains high concentrations of Hg(II),<sup>17,24</sup> transport across the tropopause is generally slow, which limits its relevance to surface deposition. However, strong convective storms can force subsidence in the surrounding clear air that can transport stratospheric ozone, and possibly stratospheric Hg(II), down into the troposphere.<sup>26,27</sup> Observations and simulations show that convective storms extending to higher altitudes have higher mercury concentrations.<sup>28,29</sup> In addition, idealized numerical models suggest that mercury scavenging efficiency is sensitive to the thermodynamic and meteorological conditions that control convective system morphology. These conditions vary regionally, and Nair et al.<sup>28</sup> found that storms forming in low-shear, high-instability environments, which frequently occur around the Gulf Coast in the summer and

Received: August 19, 2016

Revised: January 13, 2017

Accepted: January 17, 2017

Published: January 17, 2017

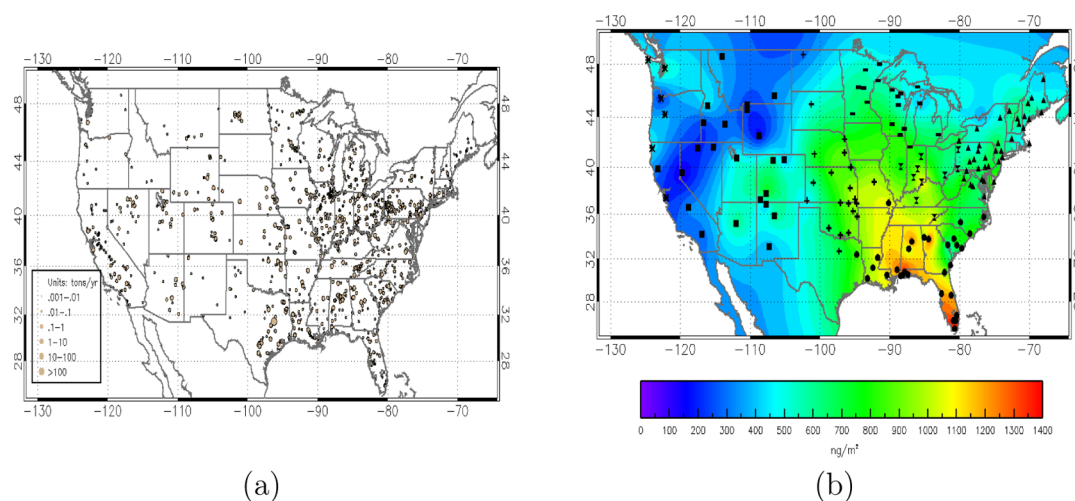


**Figure 1.** Mercury emissions, rainfall, and wet deposition over the continental United States. (a) Mercury emissions are based on the 2011 National Emissions Inventory (NEI). (b) Monthly mean mercury wet deposition for 1996–2013 is interpolated from Mercury Deposition Network (MDN) observations. Different markers indicate MDN sites associated with the seven regions discussed under *Data and Methods*: (▲) Northeast, (●) Southeast, (⊗) Ohio River Valley, (■) Midwest, (+) Great Plains, (■) Mountain West, and (\*) West Coast).

tend to produce disorganized convection, are more efficient at mercury wet removal than storms formed in some other environments.

Event-based precipitation samples provide the best opportunity to study how mercury is scavenged from the atmosphere,<sup>30</sup> but such observations are currently rare, while weekly collections are much more common. We extracted 525 event-based precipitation samples from the Mercury Deposition Network archive and used them to understand the role of storm type, as well as seasonal and geographic differences, on Hg deposition.

## DATA AND METHODS

The Mercury Deposition Network (MDN) monitors mercury wet deposition across North America with uniform analytical methods.<sup>10</sup> MDN sites are generally located in rural areas, so that measurements are regionally representative, but they may miss high deposition in urban areas or near point sources.<sup>31</sup> Most MDN sites collect weekly deposition samples, which often contain several precipitation events but sometime only one. A limited number of network sites collect precipitation samples after each precipitation event (within 24 h). Since the primary goal of this study requires event-based analysis, all MDN observations from January 2005 to August 2013 were examined to identify wet deposition measurements that come from a single precipitation system.<sup>52</sup> In order to make this determination, manual analysis of radar reflectivity and precipitation rates from U.S. National Weather Service WSR-88D radar (5 min temporal resolution level II reflectivity and level III one hour precipitation total)<sup>32,53</sup> and collocated surface rain gauges (U.S. 15 Minute Precipitation Data, created by the National Climatic Data Center)<sup>54</sup> were utilized. MDN observations were excluded if precipitation rates did not indicate a single continuous rain event. Rainfall events spanning two or more MDN collection periods were also excluded. By use of the procedure described, we found 525 wet deposition samples that could be linked to a single precipitation event (Figure 2a).

After the single-event samples are identified, radar observations are used to classify the precipitation type. We use

classification criteria developed by Smith et al.<sup>33</sup> for convective storms, with additional nonconvective categories. These radar-based criteria were chosen because they provide objective radar definitions for a comprehensive list of storm types and are appropriate for the entire United States.<sup>33</sup> The precipitation types are (1) supercell thunderstorms, which have low-level radar reflectivity values greater than 35 dBZ, a peak rotational velocity of at least 10 m/s below 7 km altitude and extending through at least one-fourth of the storm's depth, and persistence of these features for at least 10 min; (2) quasi-linear convective systems (QLCS), which have low-level reflectivity greater than 35 dBZ, length exceeding 100 km, and a length-to-width aspect ratio aspect of 3:1 or greater; (3) disorganized thunderstorms, which have low-level reflectivity greater than 35 dBZ but do not meet the requirements of supercell and QLCS categories; (4) extratropical cyclones, which are large-scale and characterized by nonconvective precipitation; (5) tropical cyclones, which are organized cyclonically rotating precipitation systems originating in the tropics; and (6) light precipitation, defined as precipitation below the 35 dBZ threshold and less than 50 km in size. While QLCS and tropical cyclones can contain both convective and stratiform precipitation, QLCS precipitation is mostly convective, whereas stratiform precipitation dominates in land-falling tropical cyclones.

For each storm type we calculate the mean precipitation depth ( $\langle p \rangle$ ) and mean deposition ( $\langle D \rangle$ ) per event (Table 1). When mercury concentration or deposition in precipitation is compared between different events, confounding effects of differences in amount of precipitation need to be taken into account. As with other soluble trace gases and aerosols, the relationship between mercury concentrations in precipitation ( $C$ ) and precipitation amount ( $p$ ) roughly follows a power-law relationship:<sup>29,34–38</sup>

$$C(p) = C_0(p/p_0)^{-\gamma} \quad (1)$$

The coefficients  $C_0$  and  $\gamma$  are fitted to observations for each precipitation type, where  $C_0$  represents the Hg concentration in an event per unit precipitation,  $p_0 = 1$  mm, and  $\gamma$  is typically positive, meaning that concentrations are diluted in large rain

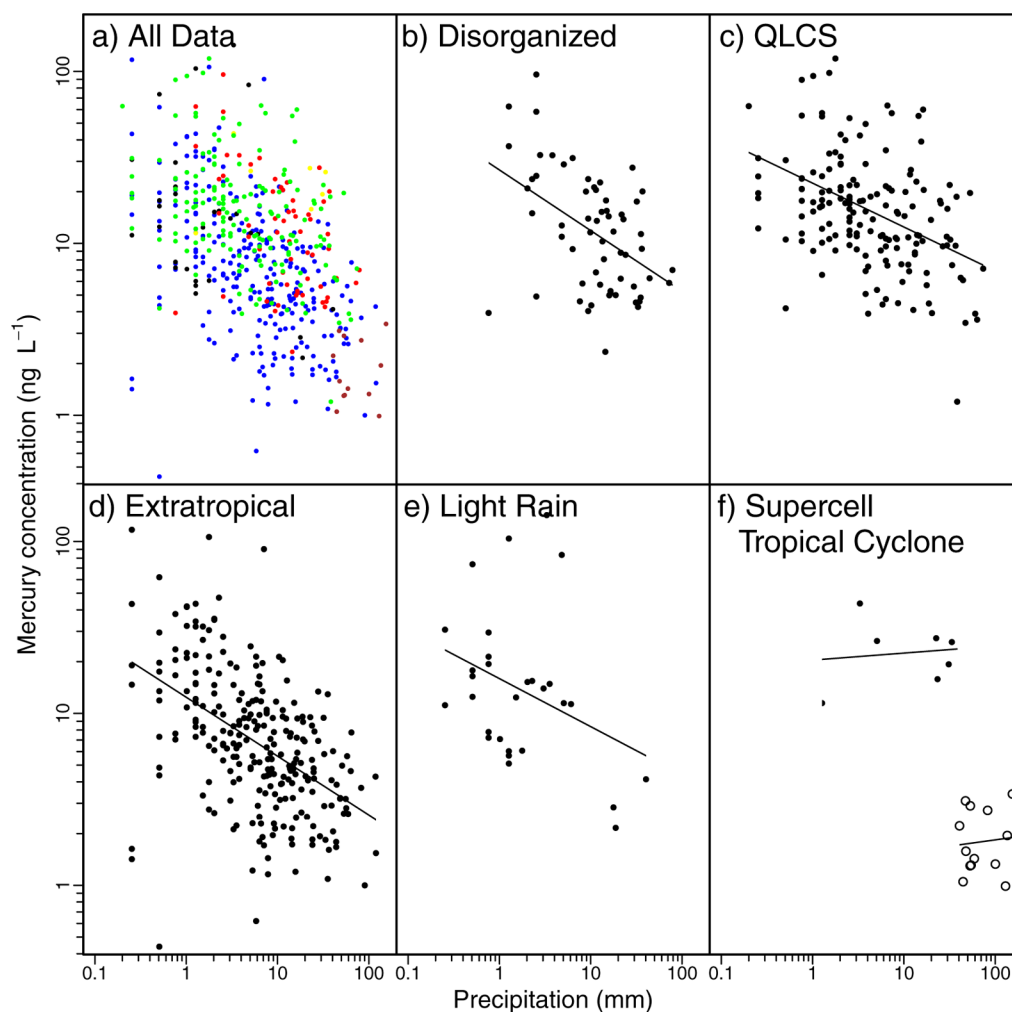


**Figure 2.** Mercury concentration versus precipitation as a function of precipitation system morphology. (a) Scatter plot of individual observations: (yellow) supercell, (red) disorganized thunderstorm, (green) QLCS, (blue) extratropical cyclone, (black) light rain, and (brown) tropical cyclone. (b–e) Mercury concentrations for (b) disorganized thunderstorm, (c) QLCS, (d) extratropical cyclones, and (e) light rain. (f) Similar plots for supercells and tropical cyclones are shown together; open circles are used to distinguish data points associated with tropical cyclones. Lines show ordinary least-squares regression described in eq 1 and summarized in Table 1.

events. The power law implies a linear relationship between  $\log(C)$  and  $\log(p)$ . In order to quantify the dilution curves for each precipitation system morphology, estimates of parameters  $\gamma$  and  $C_0$  for each type of precipitation system were determined by ordinary least-squares regression (Table 1).

Geographical and seasonal differences can also influence Hg deposition. To account for these factors, a robust linear model (RLM), implemented by use of the robustbase R package,<sup>39</sup> is constructed from observations of the individual precipitation events. The regression model is

$$D(p, i, j, k) = D_0(p/p_0)^b R_i S_j T_k \quad (2)$$

where  $D(p, i, j, k)$  is the Hg deposition resulting from precipitation depth  $p$  in region  $i$ , season  $j$ , and from storm type  $k$ ;  $D_0$  is the deposition for  $p_0 = 1$  mm precipitation;  $R_i$  is a multiplicative factor for region  $i$ ;  $S_j$  is a multiplicative factor for season  $j$ ; and  $T_k$  is a multiplicative factor for storm type  $k$ . The regression fit is performed on the logarithm of eq 2, which is a linear equation, and the results are transformed back (Table 2). Season, region, and storm type are all discrete predictors. Seasons are categorized as winter (December, January, and February; DJF), spring (March, April, and May; MAM),

summer (June, July, and August; JJA), and fall (September, October, and November; SON). Geographical regions are the Southeast, Mountain West, West Coast, Northeast, Ohio River Valley, Midwest, and Great Plains. The MDN sites that fall within these regions are shown in Figure 1. The RLM also tests for interactions of precipitation depth with precipitation type, season, or region, although these are not shown in eq 2 because they were not found to be significant. Interactions of precipitation type with region and season were excluded from the RLM because some precipitation types do not occur in all regions and seasons. Similarly, interactions between region and season are excluded, since observations for some combinations of these variables are not present in our data set. The optimal set of predictors is selected with a backward, stepwise model selection approach based on Akaike information criterion (AIC) implemented in the AICcmodavg R package.<sup>40</sup> This method sequentially discards predictors from the regression model to minimize the AIC value and thus identifies the most parsimonious model that maximizes the explained variability of Hg concentration with the fewest predictors.

Table 1. Mercury Concentration and Deposition for Multiple Precipitation Types<sup>a</sup>

| morphology             | <i>n</i> | <i>C</i> <sub>0</sub> (ng·L <sup>-1</sup> ) | <i>γ</i>     | <i>r</i> | <i>p</i> <sub>χ<sup>2</sup></sub> | <i>D</i> (ng·m <sup>-2</sup> ) | <i>⟨D⟩</i> (ng·m <sup>-2</sup> ) | <i>⟨p⟩</i> (mm) |
|------------------------|----------|---|--------------|----------|-----------------------------------|--------------------------------|----------------------------------|-----------------|
| supercell              | 7        | 20.4 ± 1.47*                                | -0.04 ± 0.15 | 0.12     | 0.79                              | 2800                           | 393 ± 119                        | 17.2 ± 5.16     |
| disorganized           | 61       | 26.7 ± 1.26*                                | 0.35 ± 0.09* | -0.46    | <0.01                             | 11 000                         | 182 ± 21                         | 16.8 ± 1.99     |
| QLCS                   | 160      | 22.4 ± 1.09*                                | 0.26 ± 0.05* | -0.40    | <0.01                             | 21 000                         | 133 ± 15                         | 9.26 ± 1.04     |
| extratropical cyclones | 255      | 12.4 ± 1.09*                                | 0.34 ± 0.04* | -0.59    | <0.01                             | 18 000                         | 70 ± 5                           | 12.5 ± 1.10     |
| light rain             | 29       | 15.9 ± 1.22*                                | 0.28 ± 0.15* | -0.34    | 0.06                              | 1700                           | 60 ± 21                          | 4.24 ± 1.54     |
| tropical cyclones      | 13       | 1.31 ± 3.19                                 | -0.07 ± 0.27 | 0.08     | 0.79                              | 2000                           | 154 ± 345                        | 77.1 ± 11.0     |

<sup>a</sup>*n* is the number of events, *C*<sub>0</sub> and *γ* are parameters for eq 1 with correlation coefficient *r*, *p*<sub>χ<sup>2</sup></sub> is the *p* value for the χ<sup>2</sup> goodness-of-fit test, *D* is total wet deposition, *⟨D⟩* is mean Hg deposition per precipitation event, and *⟨p⟩* is mean precipitation depth. The uncertainty ranges are standard errors for *C*<sub>0</sub>, *γ*, *D*, *⟨D⟩*, and *⟨p⟩*. Asterisk indicates statistical significance at the 0.05 level.

## RESULTS

For most storm types, mercury concentrations decline with increasing precipitation depth; however, there is large scatter apparent for all storm types in Figure 2. The scatter is due to many processes that are not explicitly accounted for in the statistical model, including initial Hg(II) concentration before the rain event, distance to Hg(II) sources, air mass trajectory, rain heterogeneity within a single storm, and other meteorological variability. Despite the scatter within the data, the power law reasonably describes the dilution effect based on χ<sup>2</sup> goodness-of-fit test (*p* ≤ 0.06 for all but tropical cyclones and supercell thunderstorms), and lack of structure (e.g., trends, skewness) in the fit residuals. The regression coefficients (Table 1) describing this dilution cluster around *γ* = 0.3 for disorganized thunderstorms, QCLS, light rain, and extratropical cyclones (all within 1 standard error, SE). This value is within the range of past dilution estimates for mercury, other trace metals, and sulfur.<sup>29,36,41</sup> The remaining storm types, supercell thunderstorms and tropical cyclones, exhibit less dilution that is statistically indistinguishable from *γ* = 0 (no dilution) but at the upper end of the coefficient uncertainty (2 SE) is also consistent with *γ* = 0.3. The data set contains few (*n* = 7, 13) of these storm types, so it is unclear whether the apparent lack of dilution in these storms reflects real differences in scavenging. The *C*<sub>0</sub> coefficients, which specify the Hg concentration in a 1 mm precipitation event, have clear differences between precipitation types (Table 1). Convective storms have the highest concentration coefficients (*C*<sub>0</sub> = 20–27 ng·L<sup>-1</sup>); light rain and extratropical cyclones have intermediate values (*C*<sub>0</sub> = 12–16 ng·L<sup>-1</sup>); and tropical cyclones have the lowest (*C*<sub>0</sub> = 1.3 ng·L<sup>-1</sup>). The uncertainties in *C*<sub>0</sub> estimates are around 1.3 ng·L<sup>-1</sup>, so these differences are statistically significant.

The mean and total deposition for each storm type is sensitive to the particular events that happen to be observed, although some patterns related to storm type emerge. The mean wet deposition (*⟨D⟩*) per event ranges from a low of 60–70 ng·m<sup>-2</sup> in extratropical cyclones and light rain to a high of 390 ng·m<sup>-2</sup> in supercell thunderstorms (Table 1). The other storm types (QLCS, disorganized thunderstorms, and tropical cyclones) have similar mean deposition of 130–180 ng·m<sup>-2</sup> per event, despite their clear differences in concentration and precipitation amount (Figure 2). In general, the storm types with high mean precipitation depth (*⟨p⟩*) tend to have high mean deposition (e.g., tropical cyclones and supercell and disorganized thunderstorms), but the tendency is weak. The tropical cyclones in our data set produced over 4 times more rain on average than the supercell storms but less than half the mean Hg deposition, because of the low Hg concentrations in these tropical cyclones. Due to the large number (*n*) of

disorganized, QLCS, and extratropical cyclones in our database, the total wet deposition from these morphologies (Table 1) contributes the majority of the total wet deposition in the events considered.

In the discussion above on the variability of mercury wet deposition as a function of precipitation system morphology, the confounding effects of geographic and seasonal variability were neglected. The RLM approach (see Data and Methods) addresses these effects, with the optimal model selected using a backward, stepwise approach. The resulting optimal RLM model has predictors of precipitation depth, season, geographic region, and precipitation system morphology. Stepwise construction of the RLM showed that the most important variable, determined by the change in AIC as predictors are removed from the RLM, is precipitation depth (ΔAIC = 534.2), followed by precipitation type (ΔAIC = 134.8), season (ΔAIC = 26.4), and region (ΔAIC = 11.6). The ΔAIC values for interactions between precipitation depth and all other predictors (season, region, and precipitation type) were positive, meaning that they degraded model performance, so these terms were excluded. The precipitation exponent *b* in eq 2 should be related to the dilution exponent *γ* in eq 1 via *b* = *γ* + 1. The value of *b* = 0.69 (log<sub>10</sub> 4.93, Table 2) is consistent with *γ* = 0.3 (Table 1) for most storm types. Since the *γ* values in Table 1 appear to differ between storm types, the lack of interaction between precipitation depth and storm type in the RLM means that the apparent differences in dilution effect (*γ*) between storm types are likely due to confounding effects of region and season. After controlling for these season and region effects, we found that all storm types have the same precipitation exponent (*b*) coefficients. Mercury emissions, transport, and atmospheric chemistry do not explicitly appear in the regression model, but they influence the baseline deposition (*D*<sub>0</sub>) through the concentrations of GOM and PBM and also influence the geographic and seasonal differences.

RLM analysis (Table 2) shows that storm morphology impacts mercury wet deposition independent of precipitation amounts, seasonality, and location. Compared to extratropical cyclones, mercury wet deposition is significantly greater in supercell thunderstorms, disorganized thunderstorms, and QLCS (*p* < 0.01). Tropical cyclone morphologies have significantly lower mercury deposition than extratropical cyclones (*p* < 0.01), and light rain is not significantly different from extratropical cyclones (*p* = 0.81). As a group, convective storms have greater mercury wet deposition than non-convective types (extratropical cyclones and light rain) by a multiplicative factor of at least 1.6 (=10<sup>*x*</sup>, where *x* ≥ 0.21 is the fit coefficient for QLCS, disorganized, or supercell; Table 2). This is similar to the factor of 1.48 ± 0.07 increase previously

Table 2. Regression Model of Hg Wet Deposition

| predictor             | value <sup>a</sup>       | std error <sup>b</sup>  | P <sup>c</sup> |
|-----------------------|--------------------------|-------------------------|----------------|
| $D_0$                 | 15.51 ng·m <sup>-2</sup> | 1.93 ng·m <sup>-2</sup> | <0.01*         |
| $b$ (precipitation)   | 0.69                     | 0.32                    | <0.01*         |
| Season (S)            |                          |                         |                |
| DJF                   | 0.62                     | 0.07                    | <0.01*         |
| MAM                   | 1.01                     | 0.09                    | 0.95           |
| JJA                   | 1                        |                         |                |
| SON                   | 0.81                     | 0.07                    | 0.01*          |
| Region (R)            |                          |                         |                |
| Mountain West         | 2.05                     | 0.71                    | 0.02*          |
| Great Plains          | 1.28                     | 0.17                    | 0.05*          |
| Midwest               | 1.03                     | 0.11                    | 0.79           |
| Southeast             | 1                        |                         |                |
| Ohio River Valley     | 0.99                     | 0.11                    | 0.92           |
| Northeast             | 0.74                     | 0.07                    | <0.01*         |
| West Coast            | 0.69                     | 0.31                    | 0.31           |
| Storm Type (T)        |                          |                         |                |
| supercell             | 2.54                     | 0.71                    | <0.01*         |
| disorganized          | 1.68                     | 0.20                    | <0.01*         |
| QLCS                  | 1.62                     | 0.15                    | <0.01*         |
| light rain            | 1.04                     | 0.18                    | 0.81           |
| extratropical cyclone | 1                        |                         |                |
| tropical cyclone      | 0.57                     | 0.09                    | <0.01*         |

<sup>a</sup>All values are unitless except  $D_0$ . Values for season, region, and storm type are multiplicative factors. Values are defined as 1 for the reference season (JJA), region (Southeast), and storm type (extratropical cyclone). <sup>b</sup>Standard error of regression parameter values. <sup>c</sup> $P$  is the probability that the coefficient value is 0 (for precipitation  $b$ ) or 1 (for all others, which is 0 in log transform). For the discrete categorical variables, this determines whether the season, region, or storm type differs from the reference category. Asterisk indicates statistical significance at the 0.05 level.

found for summer thunderstorms in the eastern United States.<sup>29</sup>

After control for precipitation depth, region, and morphology, the RLM analysis (Table 2) shows that wet deposition is highest during summer and lowest during the winter. For a given precipitation amount, storm type, and season, mercury wet deposition is also highest over the Mountain West region, followed by the Great Plains, then by a group consisting of the Southeast, Midwest, and Ohio River Valley (Table 2). The lowest deposition after controlling for other factors is found in the Northeast and West Coast. Relative to the Southeast, the differences are statistically significant only for the Mountain West ( $p = 0.02$ ), Northeast ( $p < 0.01$ ), and Great Plains ( $p = 0.05$ ).

## DISCUSSION

We have identified samples in the MDN archive that originate from single precipitation events, providing the most geographically diverse database of mercury wet deposition events to date. After accounting for dilution effects, we find that the variability of mercury concentrations in rainfall is best explained by precipitation system morphology, season, and region. The regression model shows that mercury deposition tends to be greater in convective precipitation than in stratiform precipitation, greater in summer than winter, and greater in the high-elevation regions of the western states than the rest of the United States.

The following discussion considers the processes that are consistent with statistical differences in mercury deposition

between seasons, regions, and precipitation system types. Seasonal variation, with greatest deposition in summer and lowest in winter, is consistent with past studies of Hg wet deposition.<sup>10,42</sup> These have previously been attributed to the emissions, dispersion, and atmospheric chemistry that drive seasonal cycles of GOM and PBM at the surface<sup>43,44</sup> and throughout the troposphere,<sup>21</sup> as well as greater scavenging efficiency of rain than snow.<sup>45,46</sup>

Regional differences in Hg wet deposition have also been studied previously,<sup>8,10,25,47,48</sup> but our results provide some new insights. The interior western United States has lower total Hg wet deposition than the eastern United States or West Coast because of the small amounts of precipitation.<sup>10</sup> After controlling for the precipitation depth and storm type, however, we show that the Mountain West and Great Plains have the highest Hg wet deposition ( $2.0 \pm 0.3$  and  $1.3 \pm 0.14$  times higher than the Southeast, respectively; Table 2). High volume-weighted Hg concentration in precipitation has previously been observed throughout the Mountain West,<sup>10</sup> but our results, which control for precipitation depth, show that the deposition is high even after accounting for dilution. Past work has found that the free troposphere is an important source of surface GOM and PBM<sup>25,49</sup> in the western United States, and within that region, wet deposition increases with altitude.<sup>50</sup> Our results are consistent with the free troposphere as an important source of Hg wet deposition throughout the Mountain West. The same process may also enhance Hg wet deposition, to a lesser extent, at the intermediate altitudes of the United States Great Plains.

The most unique aspect of this work is that we have characterized Hg wet deposition in multiple storm types. Differences between storms remain statistically significant after we control for precipitation depth, season, and region, so we believe they represent the influence of storm dynamics and precipitation formation on wet scavenging. The convective storms have higher deposition than nonconvective storms, which has been previously seen,<sup>29</sup> because convective storms can scavenge Hg(II) from the upper and lower troposphere,<sup>28</sup> while nonconvective storms scavenge only from near the surface. Convection is not all the same, however. Deposition from supercell storms is about  $1.5 \pm 0.25$  times greater ( $= 2.5/1.7$ , Table 2) than that from disorganized thunderstorms or QLCS, although the small number of supercell storms makes it difficult to draw firm conclusions. Deposition from disorganized thunderstorms and QLCS is an additional  $1.6 \pm 0.2$  times greater than that from light rain, after control for other factors (Table 2). This pattern is consistent with organized thunderstorms having greater inflow and entrainment that resupplies Hg(II) to precipitating regions. Extratropical and tropical cyclones have much greater air inflow than thunderstorms<sup>51</sup> but lower Hg deposition, after control for other factors. This behavior may be caused by Hg(II)-depleted outflow air recirculating through the precipitating regions of these large, long-lived cyclones. Air recirculation is greater in land-falling tropical cyclones than extratropical cyclones, which is consistent with tropical cyclones having the lowest Hg deposition, after control for other factors, of any storm type investigated here.

## AUTHOR INFORMATION

### Corresponding Author

\*E-mail [kaulfusa@nsstc.uah.edu](mailto:kaulfusa@nsstc.uah.edu); phone 256-961-7326; fax 256-961-7751.

ORCID 

Aaron S. Kaulfus: 0000-0002-8319-1126

Christopher D. Holmes: 0000-0002-2727-0954

## Notes

The authors declare no competing financial interest.

## ACKNOWLEDGMENTS

This study was sponsored by Southern Company Graduate Research Internship and University of Alabama in Huntsville Industry/University Cooperative Graduate Student Research Program (IUCGSRP 14-068) and NSF CAREER Grant AGA-1352046. We are thankful for the valuable suggestions from the three anonymous reviewers that resulted in substantial improvements of the manuscript.

## REFERENCES

- (1) Zahir, F.; Rizwi, S. J.; Haq, S. K.; Khan, R. H. Low dose mercury toxicity and human health. *Environ. Toxicol. Pharmacol.* **2005**, *20*, 351–60.
- (2) Mergler, D.; Anderson, H. A.; Chan, L. H. M.; Mahaffey, K. R.; Murray, M.; Sakamoto, M.; Stern, A. H. *Ambio* **2007**, *36*, 3–11.
- (3) Scheuhammer, A. M.; Meyer, M. W.; Sandheinrich, M. B.; Murray, M. W. Effects of Environmental Methylmercury on the Health of Wild Birds, Mammals, and Fish. *Ambio* **2007**, *36*, 12–18.
- (4) Sunderland, E. M. Mercury exposure from domestic and imported estuarine and marine fish in the U.S. seafood market. *Environ. Health Perspect.* **2007**, *115*, 235–242.
- (5) Zhang, H.; Feng, X.; Larssen, T.; Qiu, G.; Vogt, R. D. In inland China, rice, rather than fish, is the major pathway for methylmercury exposure. *Environ. Health Perspect.* **2010**, *118*, 1183–1188.
- (6) Gratz, L. E.; Keeler, G. J.; Morishita, M.; Barres, J. a.; Dvonch, J. T. Assessing the emission sources of atmospheric mercury in wet deposition across Illinois. *Sci. Total Environ.* **2013**, *448*, 120–31.
- (7) Lai, S.; Holsen, T.; Hopke, P.; Liu, P. Wet deposition of mercury at a New York state rural site: Concentrations, fluxes, and source areas. *Atmos. Environ.* **2007**, *41*, 4337–4348.
- (8) Zhang, Y.; Jaegle, L. Decreases in mercury wet deposition over the united states during 2004–2010: Roles of domestic and global background emission reductions. *Atmosphere* **2013**, *4*, 113–131.
- (9) Shanley, J. B.; Engle, M. a.; Scholl, M.; Krabbenhoft, D. P.; Brunette, R.; Olson, M. L.; Conroy, M. E. High Mercury Wet Deposition at a "clean Air" Site in Puerto Rico. *Environ. Sci. Technol.* **2015**, *49*, 12474–12482.
- (10) Prestbo, E. M.; Gay, D. a. Wet deposition of mercury in the U.S. and Canada, 1996–2005: Results and analysis of the NADP mercury deposition network (MDN). *Atmos. Environ.* **2009**, *43*, 4223–4233.
- (11) Selin, N. E.; Jacob, D. J. Seasonal and spatial patterns of mercury wet deposition in the United States: Constraints on the contribution from North American anthropogenic sources. *Atmos. Environ.* **2008**, *42*, 5193–5204.
- (12) Seigneur, C.; Lohman, K.; Vijayaraghavan, K.; Shia, R.-L. Contributions of global and regional sources to mercury deposition in New York State. *Environ. Pollut.* **2003**, *123*, 365–373.
- (13) Guentzel, J. L.; Landing, W. M.; Gill, G. A.; Pollman, C. C. Processes Influencing Rainfall Deposition of Mercury in Florida. *Environ. Sci. Technol.* **2001**, *35*, 863–873.
- (14) Schroeder, W. H.; Munthe, J. Atmospheric Mercury. An Overview. *Atmos. Environ.* **1998**, *32*, 809–822.
- (15) Holmes, C. D.; Jacob, D. J.; Corbitt, E. S.; Mao, J.; Yang, X.; Talbot, R.; Slemr, F. Global atmospheric model for mercury including oxidation by bromine atoms. *Atmos. Chem. Phys.* **2010**, *10*, 12037–12057.
- (16) Swartzendruber, P. C.; Jaffe, D. A.; Prestbo, E. M.; Weiss-Penzias, P.; Selin, N. E.; Park, R.; Jacob, D. J.; Strobe, S.; Jaeglé, L. Observations of reactive gaseous mercury in the free troposphere at the Mount Bachelor Observatory. *J. Geophys. Res.* **2006**, *111*, No. D24301.
- (17) Lyman, S. N.; Jaffe, D. A. Formation and fate of oxidized mercury in the upper troposphere and lower stratosphere. *Nat. Geosci.* **2012**, *5*, 114–117.
- (18) Sillman, S.; Marsik, F. J.; Al-Wali, K. I.; Keeler, G. J.; Landis, M. S. Reactive mercury in the troposphere: Model formation and results for Florida, the northeastern United States, and the Atlantic Ocean. *J. Geophys. Res.* **2007**, *112*, No. D23305.
- (19) Slemr, F.; Ebinghaus, R.; Brenninkmeijer, C. a. M.; Hermann, M.; Kock, H. H.; Martinsson, B. G.; Schuck, T.; Sprung, D.; van Velthoven, P.; Zahn, a.; Ziereis, H. Gaseous mercury distribution in the upper troposphere and lower stratosphere observed onboard the CARIBIC passenger aircraft. *Atmos. Chem. Phys. Discuss.* **2008**, *8*, 18651–18688.
- (20) Talbot, R.; Mao, H.; Scheuer, E.; Dibb, J.; Avery, M. Total depletion of Hg<sup>0</sup> in the upper troposphere-lower stratosphere. *Geophys. Res. Lett.* **2007**, *34*, No. L23804.
- (21) Brooks, S.; Ren, X.; Cohen, M.; Luke, W. T.; Kelley, P.; Artz, R.; Hynes, A.; Landing, W.; Martos, B. Airborne vertical profiling of mercury speciation near Tullahoma, TN, USA. *Atmosphere* **2014**, *5*, 557–574.
- (22) Gratz, L. E.; Ambrose, J. L.; Jaffe, D. A.; Shah, V.; Jaeglé, L.; Stutz, J.; Festa, J.; Spolaor, M.; Tsai, C.; Selin, N. E.; et al. Oxidation of mercury by bromine in the subtropical Pacific free troposphere. *Geophys. Res. Lett.* **2015**, *42*, 10494–10502.
- (23) Shah, V.; Jaeglé, L.; Gratz, L. E.; Ambrose, J. L.; Jaffe, D. A.; Selin, N. E.; Song, S.; Campos, T. L.; Flocke, F. M.; Reeves, M.; et al. Origin of oxidized mercury in the summertime free troposphere over the southeastern US. *Atmos. Chem. Phys.* **2016**, *16*, 1511–1530.
- (24) Murphy, D. M.; Hudson, P. K.; Thomson, D. S.; Sheridan, P. J.; Wilson, J. C. Observations of mercury-containing aerosols. *Environ. Sci. Technol.* **2006**, *40*, 3163–3167.
- (25) Weiss-Penzias, P.; Amos, H. M.; Selin, N. E.; Gustin, M. S.; Jaffe, D. a.; Obrist, D.; Sheu, G. R.; Giang, a. Use of a global model to understand speciated atmospheric mercury observations at five high-elevation sites. *Atmos. Chem. Phys.* **2015**, *15*, 1161–1173.
- (26) Škerlak, B.; Sprenger, M.; Wernli, H. A global climatology of stratosphere-troposphere exchange using the ERA-Interim data set from 1979 to 2011. *Atmos. Chem. Phys.* **2014**, *14*, 913–937.
- (27) Pan, L. L.; Homeyer, C. R.; Honomichl, S.; Ridley, B. a.; Weisman, M.; Barth, M. C.; Hair, J. W.; Fenn, M. a.; Butler, C.; Diskin, G. S.; Crawford, J. H.; Ryerson, T. B.; Pollack, I.; Peischl, J.; Huntrieser, H. Thunderstorms enhance tropospheric ozone by wrapping and shedding stratospheric air. *Geophys. Res. Lett.* **2014**, *41*, 7785–7790.
- (28) Nair, U. S.; Wu, Y.; Holmes, C. D.; Ter Schure, A.; Kallos, G.; Walters, J. T. Cloud-resolving simulations of mercury scavenging and deposition in thunderstorms. *Atmos. Chem. Phys.* **2013**, *13*, 10143–10157.
- (29) Holmes, C. D.; Krishnamurthy, N. P.; Caffrey, J. M.; Landing, W. M.; Edgerton, E. S.; Knapp, K. R.; Nair, U. S. Thunderstorms increase mercury wet deposition. *Environ. Sci. Technol.* **2016**, *50*, 9343–9350.
- (30) Dvonch, J. T.; Keeler, G. J.; Marsik, F. J. The Influence of Meteorological Conditions on the Wet Deposition of Mercury in Southern Florida. *J. Appl. Meteor.* **2005**, *44*, 1421–1435.
- (31) Lynam, M. M.; Dvonch, J. T.; Barres, J. a.; Landis, M. S.; Kamal, A. S. Investigating the impact of local urban sources on total atmospheric mercury wet deposition in Cleveland, Ohio, USA. *Atmos. Environ.* **2016**, *127*, 262–271.
- (32) Crum, T. D.; Albery, R. L. *Bull. Am. Meteorol. Soc.* **1993**, *74*, 1669.
- (33) Smith, B. T.; Thompson, R. L.; Grams, J. S.; Broyles, C.; Brooks, H. E. Convective Modes for Significant Severe Thunderstorms in the Contiguous United States. Part I: Storm Classification and Climatology. *Wea. Forecasting* **2012**, *27*, 1114–1135.
- (34) Lindberg, S. E. Factors influencing trace metal, sulfate and hydrogen ion concentrations in rain. *Atmos. Environ.* **1982**, *16*, 1701–1709.

(35) de Pena, R. G.; Carlson, T. N.; Takacs, J. F.; Holian, J. O. Analysis of precipitation collected on a sequential basis. *Atmos. Environ.* **1984**, *18*, 2665–2670.

(36) Barrie, L. a. Scavenging ratios, wet deposition, and in-cloud oxidation: An application to the oxides of sulphur and nitrogen. *J. Geophys. Res.* **1985**, *90*, 5789–5799.

(37) Keeler, G. J.; Samson, P. J. Spatial representativeness of trace element ratios. *Environ. Sci. Technol.* **1989**, *23*, 1358–1364.

(38) Beverland, I. J.; Crowther, J. M.; Srinivas, M. S. N.; Heal, M. R. The influence of meteorology and atmospheric transport patterns on the chemical composition of rainfall in south-east England. *Atmos. Environ.* **1998**, *32*, 1039–1048.

(39) Maechler, M.; Rousseeuw, P.; Croux, C.; Todorov, V.; Ruckstuhl, A.; Salibian-Barrera, M.; Verbeke, T.; Koller, M. *robustbase: Basic Robust Statistics R package*, 2015; <http://CRAN.R-project.org/package=robustbase>.

(40) Mazerolle, M. J. *AICcmodavg: Model selection and multimodel inference based on (Q) AIC(c)*, 2015; <https://cran.r-project.org/web/packages/AICcmodavg/index.html>.

(41) Jaffrezo, J.-L.; Colin, J.-L.; Gros, J.-M. Some physical factors influencing scavenging ratios. *Atmos. Environ., Part A* **1990**, *24*, 3073–3083.

(42) Keeler, G. J.; Gratz, L. E.; Al-wali, K. Long-term Atmospheric Mercury Wet Deposition at Underhill, Vermont. *Ecotoxicology* **2005**, *14*, 71–83.

(43) Nair, U. S.; Wu, Y.; Walters, J.; Jansen, J.; Edgerton, E. S. Diurnal and seasonal variation of mercury species at coastal-suburban, urban, and rural sites in the southeastern United States. *Atmos. Environ.* **2012**, *47*, 499–508.

(44) Lan, X.; Talbot, R. W.; Castro, M.; Perry, K.; Luke, W. Seasonal and Diurnal Variations of Atmospheric Mercury across the U.S. Determined from AMNet Monitoring Data. *Atmos. Chem. Phys.* **2012**, *12*, 10569–10582.

(45) Gratz, L. E.; Keeler, G. J.; Miller, E. K. Long-term relationships between mercury wet deposition and meteorology. *Atmos. Environ.* **2009**, *43*, 6218–6229.

(46) Sigler, J. M.; Mao, H.; Talbot, R. Gaseous elemental and reactive mercury in southern New Hampshire. *Atmos. Chem. Phys. Discuss.* **2009**, *9*, 17763–17802.

(47) Lamborg, C. H.; Engstrom, D. R.; Fitzgerald, W. F.; Balcom, P. H. Apportioning global and non-global components of mercury deposition through 210Pb indexing. *Sci. Total Environ.* **2013**, *448*, 132–140.

(48) Butler, T. J.; Cohen, M. D.; Vermeylen, F. M.; Likens, G. E.; Schmeltz, D.; Artz, R. S. Regional precipitation mercury trends in the eastern USA, 1998–2005: Declines in the Northeast and Midwest, no trend in the Southeast. *Atmos. Environ.* **2008**, *42*, 1582–1592.

(49) Weiss-Penzias, P.; Gustin, M. S.; Lyman, S. N. Observations of speciated atmospheric mercury at three sites in Nevada: Evidence for a free tropospheric source of reactive gaseous mercury. *J. Geophys. Res.* **2009**, *114*, No. D14302.

(50) Huang, J.; Gustin, M. S. Evidence for a free troposphere source of mercury in wet deposition in the western United States. *Environ. Sci. Technol.* **2012**, *46*, 6621–6629.

(51) Cotton, W. R.; Alexander, G. D.; Hertenstein, R.; Walko, R. L.; McAnelly, R. L.; Nicholls, M. Cloud venting - A review and some new global annual estimates. *Earth-Sci. Rev.* **1995**, *39*, 169–206.

(52) National Atmospheric Deposition Program. *Weekly data, All MDN Sites*; <http://nadp.sws.uiuc.edu/data/MDN/weekly.aspx>, Accessed 03/14/2014.

(53) National Centers for Environmental Information, National Oceanic and Atmospheric Administration. *NEXRAD Data Archive, Inventory and Access*; <http://www.ncdc.noaa.gov/nexradinv/>

(54) National Centers for Environmental Information, National Oceanic and Atmospheric Administration. *U.S. 15 Minute Precipitation Data* (digital data set DSI-3260), archived at the National Climatic Data Center; [ftp://ftp.ncdc.noaa.gov/pub/data/15min\\_precip-3260/](ftp://ftp.ncdc.noaa.gov/pub/data/15min_precip-3260/).